The Journal of Molecular Diagnostics, Vol. 15, No. 2, March 2013

the Journal of Molecular Diagnostics
jmd.amjpathol.org

# Targeted, High-Depth, Next-Generation Sequencing of Cancer Genes in Formalin-Fixed, Paraffin-Embedded and Fine-Needle Aspiration Tumor Specimens

Andrew G. Hadd,* Jeff Houghton,* Ashish Choudhary,* Sachin Sah,* Liangjing Chen,* Adam C. Marko,* Tiffany Sanford,* Kalyan Buddavarapu,* Julie Krosting,* Lana Garmire,* Dennis Wylie,* Rupali Shinde,* Sylvie Beaudenon,* Erik K. Alexander,† Elizabeth Mambo,* Alex T. Adai,* and Gary J. Latham*

*From Asuragen, Inc.,* Austin, Texas; and the Department of Medicine,† Brigham and Women's Hospital, Boston, Massachusetts*

Accepted for publication November 13, 2012.

Address correspondence to Alex Adai, Ph.D., or Gary J. Latham, Ph.D., Asuragen, Inc., 2150 Woodward St, Suite 100, Austin, TX 78744-1038. E-mail: aadai@asuragen.com or glatham@asuragen.com.

Implementation of highly sophisticated technologies, such as next-generation sequencing (NGS), into routine clinical practice requires compatibility with common tumor biopsy types, such as formalin-fixed, paraffin-embedded (FFPE) and fine-needle aspiration specimens, and validation metrics for platforms, controls, and data analysis pipelines. In this study, a two-step PCR enrichment workflow was used to assess 540 known cancer-relevant variants in 16 oncogenes for high-depth sequencing in tumor samples on either mature (Illumina GAIIx) or emerging (Ion Torrent PGM) NGS platforms. The results revealed that the background noise of variant detection was elevated approximately twofold in FFPE compared with cell line DNA. Bioinformatic algorithms were optimized to accommodate this background. Variant calls from 38 residual clinical colorectal cancer FFPE specimens and 10 thyroid fine-needle aspiration specimens were compared across multiple cancer genes, resulting in an accuracy of 96.1% (95% CI, 96.1% to 99.3%) compared with Sanger sequencing, and 99.6% (95% CI, 97.9% to 99.9%) compared with an alternative method with an analytical sensitivity of 1% mutation detection. A total of 45 of 48 samples were concordant between NGS platforms across all matched regions, with the three discordant calls each represented at <10% of reads. Consequently, NGS of targeted oncogenes in real-life tumor specimens using distinct platforms addresses unmet needs for unbiased and highly sensitive mutation detection and can accelerate both basic and clinical cancer research. *(J Mol Diagn 2013, 15: 234—247; http://dx.doi.org/10.1016/j.jmoldx.2012.11.006)*

Next-generation sequencing (NGS) technologies have been successfully incorporated into clinical research, with numerous case studies illustrating the potential of these approaches to transform the molecular diagnosis of cancer.[1–3] As an unbiased genomic profiling method, NGS can identify common and cryptic dysregulated cellular pathways and inform both established treatment approaches and novel therapies, including treatments for rare cancers for which there are no established therapeutic guidelines.[4] Thus, NGS can reveal targets for personalized medicine that would be overlooked using available tests for oncology biomarkers.

Although accessibility to NGS technologies has burgeoned in the past few years and relatively affordable instruments, such as the Ion Torrent PGM, have helped drive this movement, there remains a paucity of published data for the application of targeted NGS of real-life cancer specimens, such as formalin-fixed, paraffin-embedded (FFPE) or fine-needle aspiration (FNA) biopsy specimens. FFPE and FNA specimens are integral to the diagnosis of virtually every suspected cancer case, and the estimated hundreds of millions of archived samples can provide a wealth of molecular information about disease progression and treatment.[5,6] To practically enable the

Supported, in part, by a Cancer Prevention Institute of Texas grant (CP120017) and Asuragen, Inc.

Disclosures: A.G.H., J.H., A.C., S.S., L.C., A.C.M., T.S., K.B., J.K., L.G., D.W., R.S., S.B., E.M., A.A., and G.J.L. were employees of Asuragen, Inc., and held stock or stock options in the company when the work was performed.


http://dx.doi.org/10.1016/j.jmoldx.2012.11.006

analysis of these specimens, NGS technologies must be compatible with small quantities of potentially fragmented and cross-linked DNA. The well-established performance of PCR with such clinical samples in other mutation assays[7] suggests that the targeted enrichment of specific gene regions using PCR is well suited to process such samples before NGS.

Molecular analyses of cancer specimens must also address cellular heterogeneity (ie, mixtures of tumor and stroma) and/or molecular heterogeneity (ie, subclones of varying genotype).[8–10] Indeed, the poor long-term treatment efficacy of many cancers is best explained by therapy-resistant subclones or mutations present within the primary tumor.[8,11,12] As a result, NGS technologies must also balance breadth of content with sequencing depth to reveal low-abundance mutations that may be clinically relevant.

Our approach was to carefully assess high depth (ie, >1000 reads per target) NGS with residual clinical FFPE and FNA samples and to compare and contrast enrichment workflows between an Illumina GAIIx and an Ion Torrent PGM. The GAIIx represents an established and more commonly used sequencing-by-synthesis methodology with high capacity and >100-nucleotide (nt) read lengths.[13] The PGM represents an emerging NGS approach that relies on non-optical semiconductor sequencing technology with a rapid turnaround time.[14] We designed and evaluated a PCR-based workflow to selectively amplify 540 mutational hot spots within 35 amplicons targeting 16 cancer-relevant genes. A subset of 9 amplicons within this panel, using the same primer designs and PCR conditions, was also investigated and used for residual clinical samples analyzed on the PGM. A quality control procedure was integrated to assess DNA quality and amplicon yield before NGS analysis on either platform. This approach maximized assessment of common variants between platforms, conserved precious clinical DNA samples, and allowed for an increase in sample capacity per run, relevant to higher-throughput cancer gene characterization for highly informative variants. As a result, this study addresses key requirements for the adoption of targeted NGS methods across different instrument platforms for routine testing in the clinical laboratory.

## Materials and Methods

### Overview of Sample Cohort, Cancer Gene Panel, and PCR Primer Design

An overview of the study design, sample set, and comparator methods is shown in Figure 1. Samples were obtained from 22 characterized cell line DNA, eight individual cancer cell line DNA samples pooled into a single positive control, 38 FFPE tissue specimens from colorectal cancer (CRC) resections, and 10 FNA specimens from thyroid nodules. Unless otherwise specified, all samples were quantified using a NanoDrop spectrophotometer (ThermoScientific, Wilmington, DE) and normalized to 10 ng/μL in deionized water before PCR.

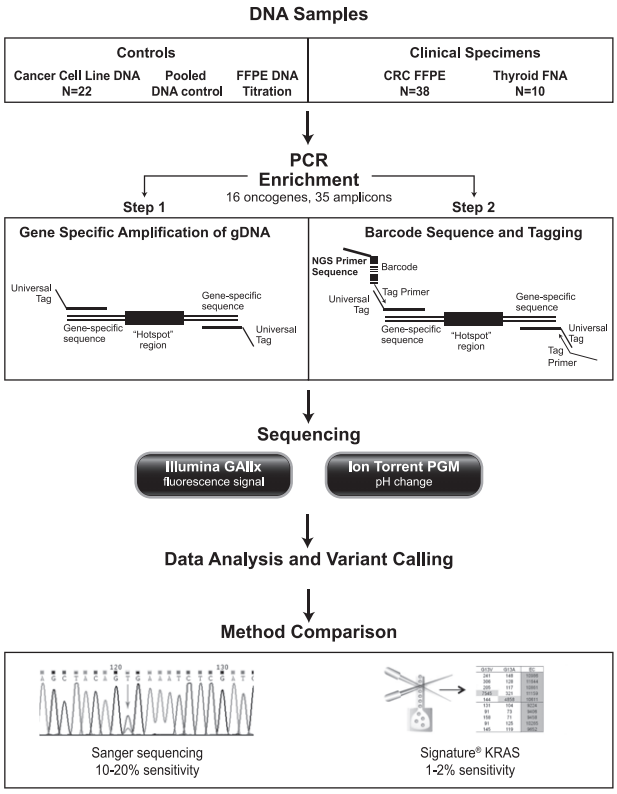


**Figure 1** Study design and workflow schematic for PCR enrichment, platform testing, data analysis, and comparison methods. DNA samples, sourced from human and cancer cell lines, FFPE tumor biopsy specimens, and thyroid FNA specimens were prepared for either GAIIx or PGM analysis using a two-step PCR with loci-specific amplification, followed by a second PCR to append instrument-specific adapters and barcodes. A training set of human and cancer cell line DNA, a pooled DNA-positive control, and a titration of FFPE specimens were used to develop bioinformatic pipelines for data analysis. The results were compared with Sanger sequencing and Signature KRAS analysis as conventional reference methods.

The general workflow for sample preparation, shown in Figure 1, included a two-step PCR procedure to amplify 35 regions within 16 oncogenes (listed in Table 1) and append platform-specific sequencing adapters. The gene-specific primers were designed to generate amplicon read regions of 61 to 80 bp according to previously published designs.[15] This oncogene panel of 35 amplicons encompassed 1283 nt, 168 db single-nucleotide polymorphism identifiers (v. 132) and 540 COSMIC (v. 57) database records, which represented >95% of all mutations reported within these 16 genes.[16] A specific subpanel of nine loci in *KRAS*, *BRAF*, *HRAS*, *NRAS*, and *PIK3CA*, using the same PCR primers and reaction conditions from the 35-amplicon panel, were selected for PGM analysis of residual clinical samples (Table 1). This subpanel encompassed 487 nt and included 222 unique variants representing >95% of variants reported in the COSMIC database for these genes.[16] COSMIC database variants covered in either the 35- or 9-amplicon panel are presented in Supplemental Table S1. Only 10 ng of DNA was required for the 9-amplicon panel compared

**Table 1** Oncogene targets and codon regions from 35 amplicons spanning 16 genes for PCR enrichment and NGS analysis

| Gene | Codons | Gene | Codons |
|---|---|---|---|
| *ABL1* | 249–258 | *HRAS* | **9–20** |
| | 315–324 | | **59–65** |
| *AKT1* | 16–27 | *JAK2* | 607–618 |
| *BRAF* | 591–599 | *KIT* | 557–569 |
| | **600–610** | | 566–579 |
| *EGFR* | 709–722 | | 815–826 |
| | 757–761 | *KRAS* | **4–15** |
| | 788–798 | | **55–65** |
| | 737–749 | | 137–148 |
| | 744–754 | *MET* | 1245–1256 |
| | 767–779 | *NRAS* | **9–20** |
| | 849–861 | | **55–67** |
| *FGFR1* | 124–132 | *PDGFRA* | 560–572 |
| | 250–262 | | 840–852 |
| *FGFR3* | 249–254 | *PIK3CA* | **540–551** |
| | 363–374 | | **1038–1049** |
| | 638–650 | *RET* | 916–926 |
| *FLT3* | 829–840 | | |

The codon range corresponded to the sequenced region in the amplicon for that gene. A subpanel of 5 genes and 9 amplicons (bold) was used for single-well PCR enrichment and analysis of clinical samples on the PGM.

with 50 ng for the larger panel. An overview of the sample cohort is presented in Supplemental Table S2.

## Preparation of Cell Line DNA Samples and a Pooled DNA-Positive Control

Cell line DNA samples that were characterized in the HapMap project, including NA12156, NA12878, NA18507, and NA19240, were obtained from the Coriell Cell NIGMS repository (Coriell, Hampton, NJ). DNA samples isolated from 18 cancer cell lines, listed in Supplemental Table S3, were donated by Dr. David Sidransky (Johns Hopkins University, Baltimore, MD). A pooled positive control was generated with DNA from eight cancer cell lines mixed at mass fractions ranging from 2% to 35% (assuming diploidy). This pooled DNA positive control contained DNA from the following cell lines: A-549 (35%), MIA PaCA-2 (20%), T24 (10%), RKO (15%), SK-Mel-2 (7%), HCT116 (6%), and SW1116 (2%), obtained from ATCC (Manassas, VA), and GP2d (5%), obtained from HPA Culture Collections (Salisbury, UK).

## FFPE Sample Preparation and Characterization

FFPE tissue specimens from stage II colon tumors were acquired in accordance with appropriate human subject regulations. DNA was isolated using the RecoverAll Total Nucleic Acid Isolation Kit for FFPE (Life Technologies, Foster City, CA), according to the manufacturer's instructions. Before NGS analysis, PCR products in hot spot regions for *KRAS*, *BRAF*, and *PIK3CA* genes were analyzed using Sanger sequencing. PCR primer sequences and reaction conditions specific to each target region are listed in Supplemental Table S4. *KRAS* PCR products were sent to ACGT (Wheeling, IL) for sequencing. *BRAF* and *PIK3CA* PCR products were sent to the ICMB Core Facilities at the University of Texas at Austin for sequencing. All sequence traces were analyzed using DNATools Xplorer, version 2.4.2 (DNATools, Inc., Fort Collins, CO). These samples were also assessed before NGS analysis using Signature KRAS (Asuragen, Inc., Austin, TX), a liquid bead array method on a Luminex platform for detection of seven KRAS codon 12 and 13 variants.[17] Based on outcomes of Sanger sequencing and Signature KRAS analysis, extracted DNA from three of these FFPE specimens were used to generate a twofold dilution series of known mutant DNA in a background of wild-type DNA for the same hot spot locus. One CRC sample failed read quality control metrics on the GAIIx and PGM and was omitted from analysis.

## Thyroid FNA Sample Preparation and Characterization

Thyroid FNA biopsy specimens were obtained from Brigham and Women's Hospital (Boston, MA) under Institutional Review Board–approved study protocols. On collection, ultrasonographic-guided aspirations were placed immediately in 1 mL of RNARetain RNA Stabilization Solution (Asuragen, Inc., Austin, TX) and then shipped on ice to Asuragen, Inc., for analysis. Total nucleic acids were isolated from the FNA biopsy specimens using the PARIS Kit (Life Technologies, Foster City, CA) optimized for samples preserved in RNARetain solution (Asuragen, Inc.).

## PCR Enrichment for Illumina GAIIx Analysis

DNA samples were enriched for GAIIx analysis using a two-step PCR process that included gene-specific primers and a tagging PCR to append barcode sequences and Illumina-specific adapters (Figure 1). PCR primers included an approximately 20-nt gene–specific sequence and either a 17-nt GAIIx-specific tag on the 5′-end of the forward primer (5′-CGCTCTTCCGATCTCTG-3′) or a 17-nt GAIIx-specific tag on the 5′-end of the reverse primer (5′-TGCTCTTCCGATCTGAC-3′). To generate size-resolved PCR products, the PCR primers were subdivided into five separate pools of seven-plex PCRs per sample, as shown in Supplemental Table S5. The PCR cycling conditions were 95°C for 5 minutes and 45 cycles of 95°C for 30 seconds, 55°C for 30 seconds, and 72°C for 1 minute. The tagging PCR was completed using a 1-μL aliquot of the gene-specific PCR product and 95°C for 5 minutes and 10 cycles of 95°C for 30 seconds, 55°C for 30 seconds, and 72°C for 1 minute. The forward primer was 5′-AATGATACGGCGACCACCGAGATCTACACTCTTTCCCTACACGACGCTCTTCCGATCTCTG-3′, and the reverse primer was 5′-CAAGCAGAAGACGGCATACGAGATNNNNNNGTGACTGGAGTTCAGACGTGTGCTCTTCCGATCTGAC-3′, where

NNNNNN corresponded to the reverse complement of the six-nucleotide barcode sequence. The three nucleotides at the 3′-end of each primer were used to confer target-strand specificity on the forward and reverse primers. Up to 68 barcode sequences, listed in Supplemental Table S6, were available from the manufacturer (Illumina) or generated using Barcrawl.[18] A forward primer complementary to the adapter region included a 6-carboxyflourescein (FAM) label for capillary electrophoresis (CE) analysis of the unpurified PCR products from each of the multiplex PCRs. CE analysis was completed on a 3500xl Genetic Analyzer (Life Technologies) using a 50-fold dilution of the PCR products and sizing with a ROX 400-HD ladder (Life Technologies).

Adapter-tagged PCR products were pooled and purified using AMPure XP (Beckman Coulter, Indianapolis, IN) and quantified using the KAPA Library Quant kit (KAPA Biosystems, Cape Town, South Africa), according to manufacturer's guidelines. All samples were normalized to 20 nmol/L and pooled into respective multiplexed mixtures comprising 24 to 68 samples per lane, depending on the experimental design. Flow cell preparation and data acquisition were completed following manufacturer-recommended protocols, except that cluster definition was achieved using cycles 4 to 9 to mitigate processing errors from the first three common nucleotides, C-T-G, in the PCR products. All sequencing runs were performed as single reads of 101 bp plus 7-bp index sequence reads using 3 TruSeq, version 5.0, 36-bp read sequencing kits per run (Illumina).

### PCR Enrichment for Ion Torrent PGM Analysis

PCR enrichment for Ion Torrent PGM analysis of the 1283-nt region, corresponding to 35 amplicons in 16 genes, followed a similar procedure as described for the GAIIx, except that the gene-specific primers included a 5′-TACGACTCACTATAGGGAGA-3′ sequence on the forward primer and a 5′-CCTCTCTATGGGCAGTCGGTGAT-3′ on the reverse primer. To append adapter-specific sequences on these primers, the forward tagging primer for the PGM was 5′-CCATCTCATCCCTGCGTGTCTCCGACTCAGNNNNNNTACGACTCACTATAGGGAGA-3′, where NNNNNN corresponded to specific index sequences listed in Supplemental Table S7. A single-well multiplex PCR corresponding to nine regions within five genes (Table 1) was used to prepare amplicons from CRC FFPE and thyroid FNA DNA samples for analysis on the PGM. These PCR products were generated using the same gene-specific primer pairs in one panel plus two other primer pairs previously evaluated in the 35-amplicon panel. Amplicons were quantified using a NanoDrop Spectrophotometer or a high-sensitivity DNA chip on a Bioanalyzer (Agilent Technologies, Santa Clara, CA). Approximately 500 to 700 million copies were input for manual emulsion PCR, and approximately 100 to 150 million copies of templates were used for the Ion One Touch (Life Technologies) automated emulsion PCR. The positive Ion Sphere Particles were recovered and enriched according to the manufacturer's procedures. Sequencing data were obtained using a 100-bp sequencing kit and either a 314 (1.3 million wells) or a 316 (6.3 million wells) chip indexed from 5 to 18 samples per run.

### GAIIx and PGM Data Processing Bioinformatics

The sequence read data generated from the GAIIx were demultiplexed, trimmed of adapter and primer sequences, and then filtered for high-quality reads by retaining only the files in which >90% of the bases had quality scores of 17 or higher. Alignments were performed using the Burrows-Wheeler Aligner (0.5.9-r16)[19] against the human genome (19) sequence and processed using a GATK-based workflow (1.3-21) to add read group information; perform local realignment, particularly around insertions and deletions; recalibrate Q scores; and estimate Per-Base Alignment Quality scores, as previously described.[20] Data collected on the PGM were collated and reanalyzed using the Torrent Suite 1.5.1 using FASTQ files from the Ion Torrent Browser. High-quality read files (ie, a quality score >17 for the whole read and trimmed of adapter, barcode, and primer sequences) were aligned using either Burrows-Wheeler Aligner or TMAP, version 0.1.3, and further processed using a variant calling work flow similar to the Illumina-generated files.

Automated variant calling, using a customized variant caller pipeline, was achieved using statistical probabilities for each nucleotide, filtering nucleotide positions of high background and frequency from training samples, applying a background variant threshold for each sample type and platform, and enforcing a coverage filter on the read depth relative to the median reads for that sample. Variant calls were achieved after hypothesis testing at each base position using an analysis that aggregated statistics for the frequency of nontarget base calls. The *P* value of the corresponding statistical test was then Phred scaled and defined as a variant call score. The threshold for making a positive call using this value was determined empirically.

Threshold estimates for the call scores were calibrated on the GAIIx based on results from individually sequencing 22 cell lines, including eight with previously published mutation data. The variant caller strategy was tuned for greater sensitivity at the risk of a reduced positive predictive value. These samples were used to establish basic rules for variant calling, including locating and filtering sites that have high background and establishment of thresholds for percentage variant and variant caller score below which all calls would be negative. The high background sites were defined as those sites that had coverage within 10-fold of the median for a given training set sample (any of the 22 cell line samples) and were not expected to be mutants, yet had an observed percentage variant >2% in at least 2 of the 22 samples. Only nine high background sites were flagged (<1% of the total covered space). The variant caller score threshold was simply

the maximum of 1000 or the 99th percentile score for a given sample. The background threshold score was set at the maximum of 2% or the 99$^{th}$ percentile for cell lines (or high-quality DNA), and the maximum of 4% or the 99$^{th}$ percentile for FFPE (or lower-quality DNA). By resubstituting these parameters on the 22 cell lines, we observed 100% sensitivity (eight of eight detected) without any false positives, with the caveat that these performance estimates were based on training and testing of the same samples (Supplemental Table S3). A similar procedure was used for the PGM data, with the exception that high-frequency variant sites were not filtered because these were generally eliminated using a nucleotide coverage filter, as described in *Results*.

### Platform and Method Comparison Statistics and Methods

For cell line samples analyzed using the broader 35-amplicon panel on both NGS platforms, variant calls were compared across 1283 bp. Pearson coefficients were derived in pairwise comparisons of the expected versus observed variant frequency for each of the 10 expected variants in the pooled control. For the clinical samples, NGS results between platforms were compared for nonsynonymous variants exceeding a 4% threshold and evaluated against Sanger sequencing or a liquid bead array method for accuracy, sensitivity, and specificity. Sanger sequencing results were obtained from four amplicons within three genes: i) *BRAF* codons 600 to 610, ii) *KRAS* codons 4 to 15, iii) *PIK3CA* codons 1038 to 1049, and iv) *PIK3CA* codons 540 to 551; these correspond to a total of 152 tests in 38 CRC samples (4 regions $\times$ 38). NGS results were compared with a liquid bead assay of seven specific probes for variants in *KRAS* codons 12 and 13, corresponding to a total of 266 tests in 38 CRC samples (7 probes $\times$ 38).

### Confirmatory Sanger Sequencing of DNA Samples

Sequence confirmation of cell lines or clinical samples was obtained using PCR primers modified with M13 forward and M13 reverse sequences and BigDye Direct (Life Technologies), according to the manufacturer-recommended protocol. DNA sequencing reaction products were analyzed using a 3500xl Genetic Analyzer (Life Technologies) and manually scored using Chromas (Technelysium Pty Ltd, Brisbane, Australia). Results of confirmation sequencing, limited to single samples or loci prespecified from NGS analysis, were not included in the pairwise matrix for CRC sample analysis.

## Results

An overview of the study design is represented in Figure 1, which includes a description of sample specimens, PCR enrichment, and NGS processing, data analysis work flows, and method comparisons with Sanger sequencing or liquid bead array analysis. Specifically, the study was directed to address four primary objectives: i) define quality control metrics for the PCR enrichment work flow and maximize read depth and representation in FFPE and FNA samples, ii) establish qualitative and quantitative variant detection using positive controls, iii) assess mutations in FFPE and FNA specimens and compare results between NGS platforms using the appropriate variant detection methods, and iv) evaluate the potential utility of a distinct NGS chemistry as an orthogonal approach to confirm primary NGS variant calls.

### Quality Control Assessment of Amplicon Yield and Read Depth

The integration of NGS into a regulated clinical laboratory environment requires defined quality control procedures that interrogate multiple steps along the sample processing work flow and the ability to analyze challenging sample types, such as DNA from FFPE and FNA specimens. For each sample analyzed, we sought to achieve at least 1000 reads per amplicon with a uniformity of read depths within five-fold of the median to maximize the number of samples that could be multiplexed per run while accomplishing high variant detection sensitivity.

### Amplicon Quality Control before NGS Analysis

As a first step to establishing predictive quality control procedures before NGS, a high-throughput and high-resolution CE test of amplicon identity and relative quantity was implemented. Amplicons were tagged with FAM-labeled primers and designed with discrete fragment sizes to permit the resolution of each product by CE from others generated in the multiplex PCR. This CE assay was indicative of amplicon read depth by NGS (ie, the peak height of different PCR products was proportional to the read coverage observed by NGS analysis). Two examples of comparing CE peak height with NGS read depth are shown in Figure 2. In the first example, seven amplicons representing regions of KRAS, NRAS, and KIT were detected using CE, with proportional read coverage using NGS. In contrast, only three peaks were detected in a different sample because of PCR dropout of the other four target regions. A correspondingly low number of reads for the failed amplicons was observed (Figure 2B). This method provided a quality control metric before NGS analysis and a rapid method for multiplex PCR optimization without the need for an NGS readout.

### Sequencing Read Metrics for Cell Line, FFPE, and FNA Samples

We next considered the influence of different sample types on amplicon yields and read metrics. PCR enrichment and GAIIx analysis yielded median reads of 825,000 from 22 cell line samples, 932,000 from 38 FFPE samples, and 427,000 from 10 FNA samples. A representation of yields per sample

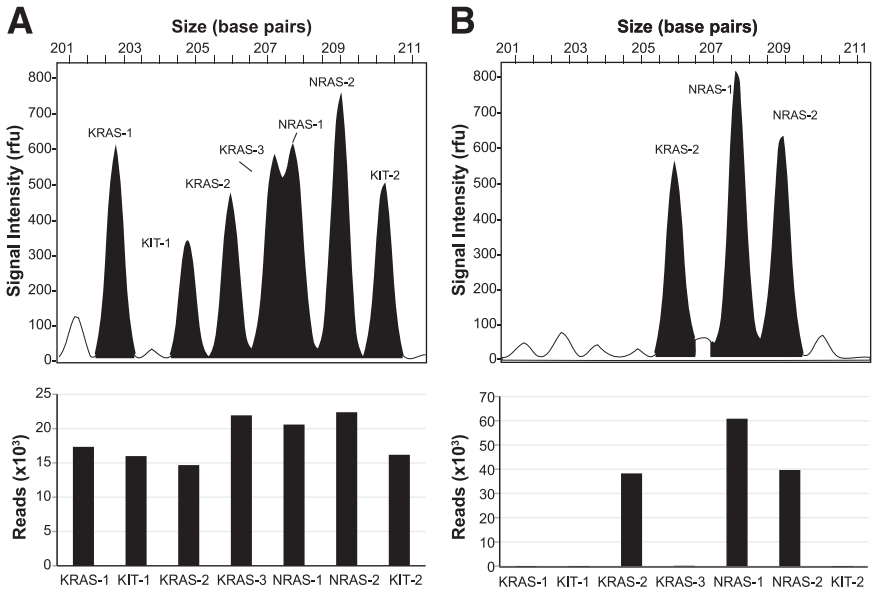


**Figure 2** CE of FAM-labeled amplicons and comparison with GAIIx read depth. Example electropherograms (**top panel**) and corresponding read coverage (**bottom panel**) for seven amplicons corresponding to regions of KRAS, KIT, and NRAS from two different cell line DNA samples. **A:** A sample yielding amplification in all seven targets detected as separate peaks by CE and corresponding read coverage for each target detected using the GAIIx. **B:** A sample with PCR dropouts detected as presence of only three of seven peaks in the electropherogram, with read coverage for only these amplicons on the GAIIx. Electropherograms were obtained from FAM-labeled PCR products separated on a 3500xl Genetic Analyzer and peak heights matched to the respective aligned reads showing regions in KRAS, KIT, and NRAS. Amplicons in the successfully amplified sample had an average of 400 ± 70 relative fluorescence units (rfu) for the peak height and 18,400 ± 3000 reads. Conversely, the amplicon dropouts identified by CE in the failed sample were the same amplicons with low read coverage after NGS.

relative to the median is shown in Figure 3A. The lower read depth from FNA specimens reflected lower DNA input because these samples were amplified from 10 ng total nucleic acids, most of which was RNA (data not shown). The read depth and uniformity were similar between sample types. The uniformity of yield across all amplicons was high, such that 97.5% of amplicons for cell line DNA, 95.2% for FFPE, and 97.3% for FNA samples were within fivefold of the median (Figure 3B). All amplicons in all samples exceeded 500 reads, and 99.8% (2444 of 2450) exceeded 1000 reads. The target amplicons were well represented in each sample type, irrespective of the sample source (Supplemental Figure S1).

By using a subset of two cell line and five FFPE DNA samples, and factoring in the capacity of the 314 chip, similar results in read coverage were observed on the PGM. The median number of high-quality reads, filtered by length (>15 nt) and quality metrics (quality score >17), was 220,000 reads for cell line DNA and 216,000 reads for FFPE DNA. The average percentage of amplicons that were within fivefold of the median (4400 reads) was 97.1% (34 of 35) for the cell line samples and 91.4% (32 of 35) for the FFPE samples. Six additional FFPE samples analyzed across three different PGM runs yielded 2000 to 7000 median reads. Overall, a high-depth was achieved in both cell line and FFPE DNA samples using the PGM to sequence products from the 35-amplicon panel.

We next considered the impact of read coverage on background variation for intact and FFPE DNA using both platforms. This assessment of background noise was used to establish variant threshold levels for the automated variant caller. Comparable results for the pooled DNA positive control and three FFPE specimens by amplicon were observed on both platforms. The GAIIx data represented amplicon sequences more consistently, whereas the PGM data revealed two to four amplicons with reads that were >10 times lower than the median number under these conditions (Figure 4A). At the 50$^{th}$ and 95$^{th}$ percentiles of the distribution of the background, variation results by platform or sample types were similar. At the 99$^{th}$ percentile, however, the variant background levels were elevated to 3% to 4% for the PGM (Figure 4B). After application of a coverage filter to remove individual nucleotide positions with <10-fold of the median reads at that position, the 99$^{th}$ percentile for all reads was reduced to 1.1% variant for FFPE DNA and 0.42% for cell line DNA. Approximately 14% of nucleotide reads for the PGM, relative to the GAIIx, were removed using this coverage filter. This filter increased the average precision from 0.185 to 0.526 on the PGM, a substantial improvement (Supplemental Table S8).

Application of platform-specific alignment parameters and, for the PGM only, a coverage filter resulted in comparable performance from the analysis of intact DNA on the two instruments. FFPE DNA, however, revealed approximately twofold elevated background variant detection at the 95$^{th}$ and 99$^{th}$ percentiles on both systems (Figure 4B). As a result, the background threshold for both platforms was initially set at 2% for cell lines or intact DNA and 4% for FFPE (or lower-quality DNA), as the result of the elevated background at the tails of the variant distribution.

## Qualitative and Quantitative Detection of Cancer-Relevant Mutations in a Pooled DNA-Positive Control and FFPE DNA Titration Series

The utility of PCR enrichment to detect known variants over a broad range of abundance was explored using a positive control from cell line DNA and a titration series of FFPE DNA

samples. We generated a multiple mutation-positive control by admixing eight cell lines to generate 10 variants, ranging from a theoretical abundance of 1% to 35%. Variants were, thus, populated across a range of relative incidence, but the mixing design intentionally emphasized the low range of abundance to more rigorously test the accuracy of variant calling in this region. The quantitative results for each cell line, target variant, expected percentage, and mutation detected are provided in Table 2. As specific examples of quantitative recovery, KRAS G12S (c.34G>A) was expected at 35% relative abundance and detected in 37% (1198 of 3251) of reads with the GAIIx and in 29% (1586 of 5441) of reads with the PGM. HRAS G12V (c.35G>T), expected at 10% abundance, was detected on the GAIIx at 13% (574 of 4413) and on the PGM at 11% (1082 of 9845). The PIK3CA H1047R mutation was reproducibly detected at 4−8% across multiple runs compared with the expected 10.5%, which may have been a component of the assumed diploidy of this variant within these cell lines. All true positive (TP) results were in the range of 2% to 35% expected abundance of variants, depending on platform. False negative (FN) results represented variants that were intentionally input at 1% abundance, which was expected given a positive call threshold of 2% for intact DNA. Furthermore, the precision-recall curve, which is a measure of the area under the curve of positive predictive value versus sensitivity, was similar for both platforms after selection of the aligner and application of the coverage filter (Supplemental Table S8).

To evaluate the quantitative detection capabilities of PCR enrichment from FFPE biopsy specimens using NGS and automated variant calling, an analytical dilution of CRC FFPE DNA containing known variants was prepared in a background of wild-type FFPE DNA. FFPE specimen 1 presented known mutations in KRAS A146T and PIK3CA H1047R, whereas FFPE specimen 2 carried a verified BRAF V600E mutation; FFPE specimen 3 had no known cancer mutations enriched within this panel. Because the relative quantity of FFPE specimen was decreased from 50% to 3.1%, a proportional decrease in the percentage of each variant was observed. This quantity-dependent response for NGS analysis of gene variants is shown in Figure 5. Five variant calls, indicated in the shaded area of Figure 5, were detected lower than the preset 4% threshold and consequently flagged as FN results. This threshold setting had an impact on balancing sensitivity and positive predictive value. At a 4% threshold, 10 calls matched to the expected variants were observed; however, there were also two unexpected calls, detected at 4.1% and 4.3% in one run of FFPE specimen 3. If the threshold was increased to 5%, then nine expected variant calls were observed without any false-positive calls. However, if the threshold was reduced to 2%, then 13 expected calls were observed, along with 18 additional false-positive calls. Thus, a 4% threshold was selected as a balance between maximizing sensitivity and minimizing the false-positive result across all nucleotides, with the understanding that low-abundance variants might be clinically meaningful and confirmation testing would be recommended.

## Targeted NGS Analysis of FFPE and FNA DNA Compares with Conventional Methods

To assess targeted NGS methodology and analysis with a range of tumor resections, 38 FFPE specimens sourced from CRC tumors and 10 FNA samples from thyroid nodules were evaluated. The samples were first enriched across 35 amplicons and analyzed using the GAIIx platform. The mutations in these samples clustered in a small set of hot spot regions within five oncogenes (*KRAS*, *HRAS*, *NRAS*, *BRAF*, and *PIK3CA*). To balance economy of analysis and to conserve limiting DNA from each sample, we used nine PCR primer pairs from the broader 35-amplicon panel to assess a 487-bp region in five genes from a single-well multiplex PCR. This more focused enrichment panel encompassed >98% of variants observed in these samples and enabled a fivefold reduction in DNA (10

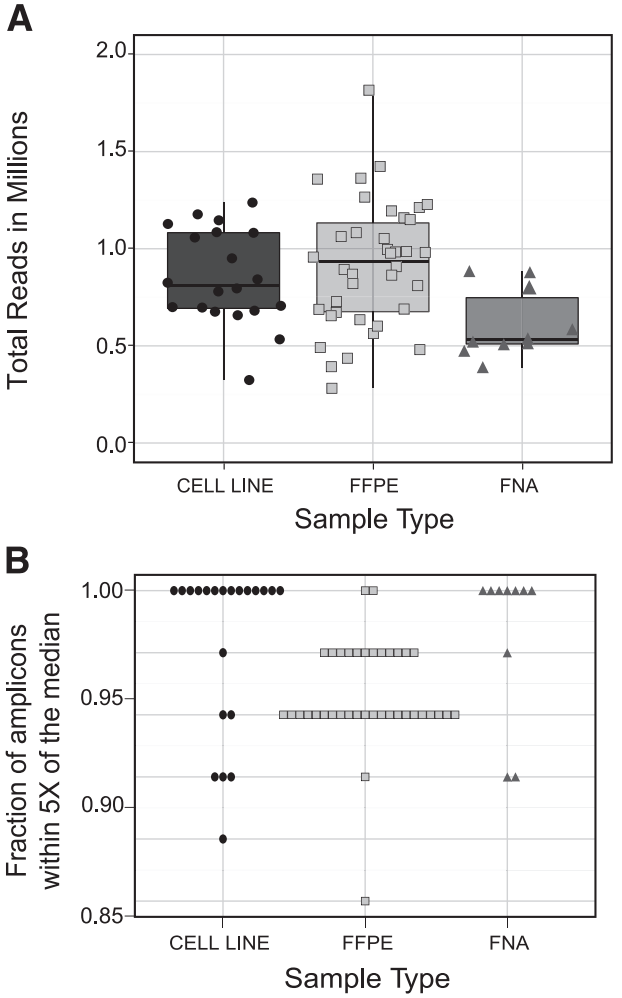


**Figure 3** Distribution of total reads, coverage per amplicon, and uniformity metrics in intact cell line, FFPE, and FNA DNA samples. **A:** Box-whisker plot corresponding to the fifth and 95$^{th}$ percentile range of the total number of mapped reads for intact, FFPE, and FNA DNA samples. **B:** The distribution of reads across 35 amplicons that were within fivefold of the median value as a representation of PCR uniformity across sample types. All samples were analyzed using the PCR enrichment method, followed by NGS on the GAIIx. Read values were normalized to 36 samples per flow cell lane equivalents.

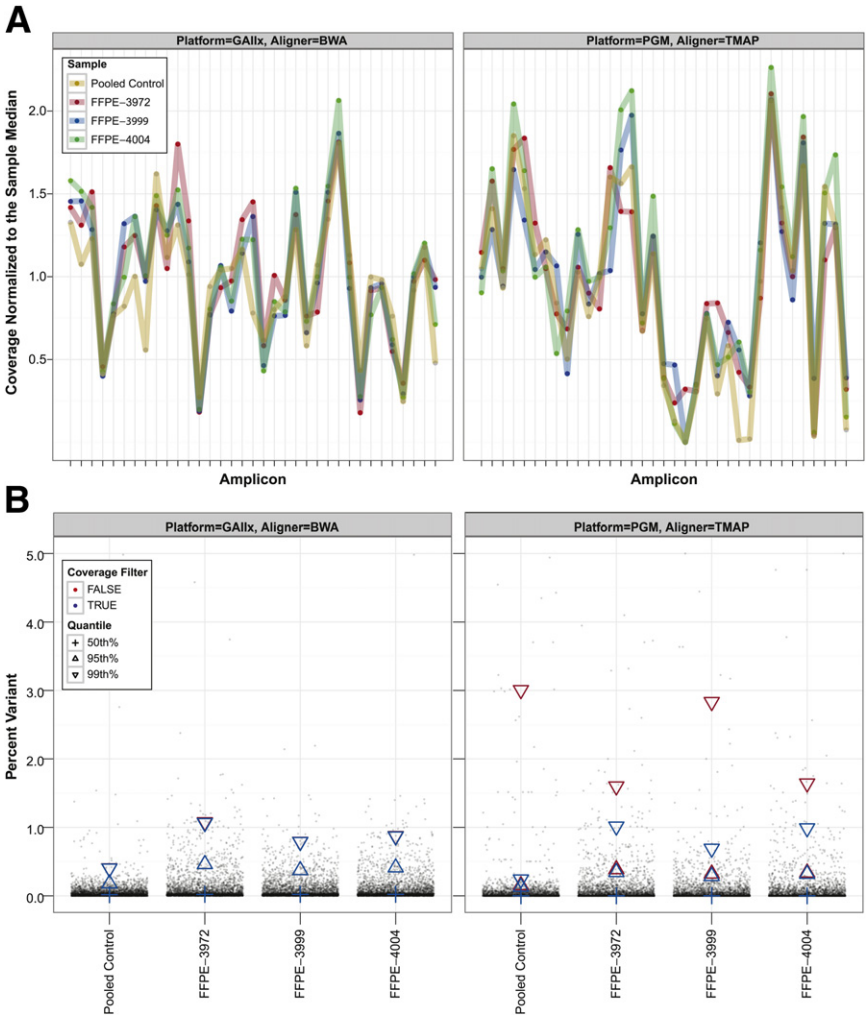


**Figure 4** Amplicon coverage and variant background assessment by NGS platform. **A:** Amplicon read depth coverage for the pooled control and three representative FFPE specimens on the GAIIx and PGM as a function of the fold change from the median read depth for 35 amplicons. **B:** The background variant distribution for the same samples at the 50$^{th}$, 95$^{th}$, and 99$^{th}$ percentiles stratified by platform, coverage filter status, and sample type. **Red triangles**, results before application of the coverage filter; **blue triangles**, results after application of a coverage filter. Application of the coverage filter, which was the removal of all positions that were not covered within 10-fold of the median, reduced the 99$^{th}$ percentile of the background on the PGM more substantially than the levels of the GAIIx. The distribution of background reads in these FFPE samples was approximately twofold higher than in the intact cell line DNA sample.

instead of 50 ng). To ensure the appropriate performance of this subpanel, we validated the subpanel for analytical sensitivity, specificity (Supplemental Table S9), and repeatability (Supplemental Table S10). The results demonstrated that the more focused enrichment panel, which shares nine primers from the 35-amplicon panel, had comparable performance to the larger target set. Results for all 38 FFPE and 10 FNA samples were obtained in three 316 chip runs performed on a single day.

## NGS Platform Comparison for Analysis of FFPE DNA from CRC Specimens

By using the GAIIx and the custom automated variant caller, the read space across 48,754-nt positions (38 samples × 1283 nt/sample) was reduced to just 43-nt variant calls of nonsynonymous variants exceeding a 4% threshold. The most common variants were KRAS G12D (8 of 38) and BRAF V600E (6 of 38). Less than three variant calls were detected in 90% of the samples. One FFPE DNA sample had five variant calls, including an expected KRAS G13D and other G>A or C>T variants present at 5% to 7% frequency. From three 316 chip runs on the PGM, a median read depth of 1700 reads per amplicon was obtained and all reads were within fivefold of the median read number per sample. A total of 32 variant calls were obtained.

An overview of the variant calls by platform compared with Sanger sequencing is shown in Figure 6A. The frequency of positive variant calls between platforms is shown in Figure 6B. We observed that the percentage variant detected on the PGM was consistently lower than the percentages on the GAIIx. The magnitude of this difference did not affect our ability to detect the underlying mutation or quantify the mutation within an accuracy range of 20% coefficient of variation. This range of variability had comparable magnitude to our repeatability study measured in multiple operators and multiple PGM instrument runs (Supplemental Table S10).

For individual FFPE specimens, 36 of 38 samples matched for overall mutation status across multiple variant regions, including detection of two complex variants, KRAS G12W (c.34_36 TGG>GGT) and NRAS Q61K (c.180_181 TC>AA). At the nucleotide level, 18,504 of 18,506 calls were concordant between platforms. Mismatched sample calls were only observed for variants representing <10% of reads. One variant call affected sample-level interpretation [namely, an NRAS Q61H (c.183 A>C) call that was

**Table 2** Analysis of the Pooled Cell Line DNA Positive Control Comparing Expected Variant Ratio with Detected Ratios, Coverage, and Variant Call Classifier for the GAIIx and PGM Platforms

| Pooled DNA mixture preparation and target variants | | | | | | NGS results by platform | | | | | | |
|---|---|---|---|---|---|---|---|---|---|---|---|---|
| | | | | | | | GAIIx | | | PGM | | |
| DNA sample | Mixing ratio (%) | Gene | Codon | Variant | Type | Expected (%) | Observed (%) | Coverage | Classifier | Observed (%) | Coverage | Classifier* |
| A-549 | 35 | *KRAS* | G12S | c.34G>A | HOM | 35 | 37 | 3251 | TP | 29 | 5441 | TP |
| MIA PaCa-2 | 20 | *KRAS* | G12C | c.34G>C | HOM | 20 | 22 | 3251 | TP | 21 | 5441 | TP |
| T24 | 10 | *HRAS* | G12V | c.35G>T | HOM | 10 | 13 | 4413 | TP | 11 | 9845 | TP |
| RKO | 15 | *BRAF* | V600E | c.1799T>A | HET | 7.5 | 7 | 7497 | TP | 8 | 4835 | TP |
| | | *PIK3CA* | H1047R | c.3140A>G | HET | 10.5† | 8 | 5837 | TP | 4 | 6415 | TP |
| SK-MEL-2 | 7 | *NRAS* | Q61R | c.182A>G | HOM | 7.0 | 12 | 7755 | TP | 9 | 6793 | TP |
| HCT 116 | 6 | *KRAS* | G13D | c.38G>A | HET | 3.0 | 1 | 3251 | FN | 2 | 5433 | TP |
| | | *PIK3CA* | H1047R | c.3140A>G | HET | 10.5† | 8 | 5837 | TP | 4 | 6415 | TP |
| GP2d | 5 | *PIK3CA* | H1047L | c.3140A>T | HET | 2.5 | 7 | 5837 | TP | 5 | 6415 | TP |
| | | *KRAS* | G12D | c.35G>A | HET | 2.5 | 5 | 3251 | TP | 3 | 5387 | TP |
| SW1116 | 2 | *KRAS* | G12A | c.35G>C | HET | 1.0 | 2 | 3251 | TP | 1 | 5387 | FN |

*TP and FP are true and false positive and TN and FN are true and false negative, respectively.
†The expected abundance is 10.5% because RKO and HTC-116 both have this mutation.

detected in 9.8% of 1141 reads on the PGM, but in only 1.8% of 26,719 reads on the GAIIx]. This NRAS variant was confirmed using Sanger sequencing (Supplemental Figure S2). Another sample with a KRAS G13D mutation was detected on both platforms, but this sample also presented a PIK3CA Q546K variant that was detected in 5% of reads on the GAIIx only (Figure 6B). This PIK3CA Q546K variant was detected in only 2.8% of 2680 reads on the PGM and was not confirmed using Sanger sequencing.

### NGS Analysis of FFPE DNA from CRC Specimens Compares with Conventional Methods

We next considered how results obtained using NGS analysis compared with conventional methods of Sanger sequencing and a mutation assay developed on a liquid bead array platform (Signature KRAS). A summary of variant calls between platform and method for each sample is listed in Supplemental Table S11. The sensitivity, TP/(TP + FN), was 100% for variants detected by Sanger. An accuracy of 96.1% (95% CI, 92.5% to 98.9%) was observed, calculated across 29 positive and 123 wild-type calls (the NRAS Q61H detected by Sanger was only confirmed on one sample after NGS analysis and not included in this matrix). The agreement matrix is summarized in Table 3. As an example of improved detection using NGS relative to Sanger sequencing, the distribution of BRAF V600E variant call frequencies is shown in Figure 6C for the 38 CRC samples. Positive calls were easily demarcated based on percentage variant. Two sequencing electropherograms are included as insets showing an indeterminate call for a sample with 17% frequency relative to a positive call for a sample with 7% frequency. The Signature KRAS assay yielded results for 266 distinct tests across seven *KRAS* loci (7 loci × 38 specimens). There were 16 positive calls from the 38 samples. The accuracy was 99.6% (95% CI, 97.9% to 100%). A single KRAS G13D variant, detected at 2000 mean fluorescence intensity using the Signature assay, was detected lower than the preset variant caller thresholds on both NGS platforms (Figure 6D).

### NGS Analysis of Thyroid FNA Specimens

To extend the applicability of NGS in multiple clinical sample types, we considered the analysis of thyroid nodule FNAs between platforms using the 35-amplicon panel on the GAIIx and the 9-amplicon panel on the PGM (Table 1). Notably, obtaining results for the GAIIx analysis of the 10 FNA specimens required a 4.5-day instrument run (1× 101 reads) and 50 ng of DNA compared with 3 hours on the PGM using only 10 ng of total nucleic acid into PCR enrichment. Thyroid cancer-relevant variants were detected in 7 of 10 samples, including three BRAF V600E mutations and a less common HRAS G13R variant. A summary of the NGS results for 10 matched FNA samples, including cytological and confirmatory Sanger sequencing results, is listed in Table 4. There was complete sample-level agreement between NGS platforms across 9 of 10 samples. The positive variants in these samples were confirmed with Sanger sequencing. In one sample, a low positive KRAS G13_V14>DI (c.38_40GCG>ACA) was detected in approximately 8% of reads using the GAIIx, but this compound mutation was neither detected on the PGM nor was it confirmed using Sanger sequencing.

## Discussion

Although previous studies have explored targeted NGS of FFPE samples,[21–23] high-depth sequencing of cancer specimens,[1–3] or the utility of novel, extremely fast NGS systems,[24–26] this is the first study, to our knowledge, that has addressed each of these issues, both qualitatively and

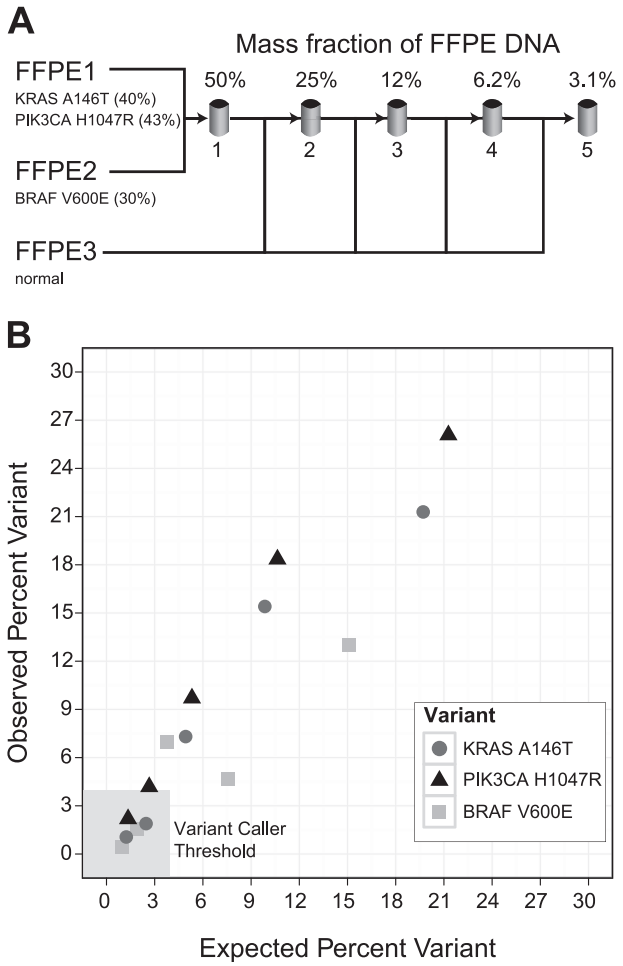


**Figure 5** Dose-dependent detection of variants within FFPE tumor DNA. **A:** Schematic preparation of a dilution series of mutation-positive FFPE specimens in a background of mutation-negative FFPE from 50% to 3.1% tumor DNA sample. FFPE specimen 1 was known to have KRAS A146T and PIK3CA H1047L, and FFPE specimen 2 presented BRAF V600E. **B:** Observed versus expected percentage variant for BRAF, PIK3CA, and KRAS variants. Values lower than the default 4% threshold were indicated in the shaded area. Two unconfirmed variant calls (data not shown) were detected at 4.1% and 4.3% in the single run of FFPE specimen 3.

quantitatively, for mutation detection in cancer across different NGS platforms. Our approach was to assess ultradeep NGS on both mature (Illumina GAIIx) and emerging (Ion Torrent PGM) platforms, after targeted PCR enrichment of standardized cancer cell line DNA mixtures and DNA from previously genotyped, residual, clinical FFPE and FNA specimens.

The larger 16-gene panel comprised 35 amplicons, 1287 bp, and at least 540 distinct mutations covering >95% of all variants within those genes. The five-gene subpanel still included >220 known variants across 487 bp and represented i) 92% of all DNA mutations reported for thyroid cancer (a disease focus of the study), ii) three of the top five mutated genes in colon cancer, and iii) gene hot spots commonly mutated in pancreatic and lung cancer, among others.[6,16] The content of both panels exceeded that of probe-based research and molecular diagnostic assays relevant to common cancers.

Although these panels cannot match the content breadth of larger panels intended for NGS that offer full exon sequencing across dozens to hundreds of cancer genes, or exome sequencing, we note that use of these larger panels comes at significant costs or trade-offs. Larger panels often require DNA inputs several times that of this study, which can prevent assessments of precious clinical DNA samples.[27] Potential gains in content breadth must be balanced with sequencing depth, cost per sample, and/or turnaround time; thus, larger panels are often sequenced more shallowly,[13] reducing analytical sensitivity, or have less favorable economics of scale or sample capacity. The additional complexity of larger panels can require more onerous validation, particularly for bioinformatics analyses and confirmatory sequencing.[28] The outcomes of our study suggest that enrichment panels of modest, but high-yield, diagnostic content are an appropriate first wave of oncology-based NGS tests for implementation in the clinical laboratory.

In this study, we used PCR enrichment and two NGS methods to identify a range of mutations at different abundances at high sensitivity in control cell line DNA and in clinical samples. Although FFPE DNA is highly modified and fragmented as a consequence of fixation and embedding, our data demonstrated comparable coverage uniformity to that of highly intact, cell line DNA. This success is likely due, in part, to the design of short PCR amplicons that minimize the amplification burden of FFPE DNA templates.[29] In our study, we used 10 ng of FFPE DNA, or approximately 3000 haploid copies, in multiplex PCRs that yielded >90% of amplicons within a fivefold range of the median read depth. This yield range was within the expected variation of PCR, which can be fourfold or greater for an input of <10,000 copies.[30] In addition, the median background variant level for FFPE DNA on either the Illumina GAIIx or Ion Torrent PGM was similar to that of cell line DNA, which was <0.05% at the 50$^{th}$ percentile, and with the appropriate analysis filters in place, only approximately 1% at the 99$^{th}$ percentile in FFPE DNA. Provided sufficient read coverage, this result is again consistent with low-level variant detection in FFPE DNA.

PCR enrichment and NGS analysis accurately recovered druggable mutations within CRC tumor biopsy specimens associated with targeted therapies, such as KRAS, BRAF, and PIK3CA. Accurate quantification of mutations in tumor biopsy specimens, especially at lower abundance, has important clinical implications and can begin to address issues of the characterization and eradication of cancer cells in heterogeneous tumors.[31,32] For example, a recently published study has demonstrated that the abundance of EGFR mutations can predict the probability of progression-free survival when patients with advanced non-small lung cancer are treated with gefitinib.[33] The application of more sensitive technologies for the detection of EGFR-pathway variants increased the identification of non-EGFR responders twofold, from 45% to 87%.[34] In this study, we demonstrated concordant detection across multiple variants using a common 4% threshold metric

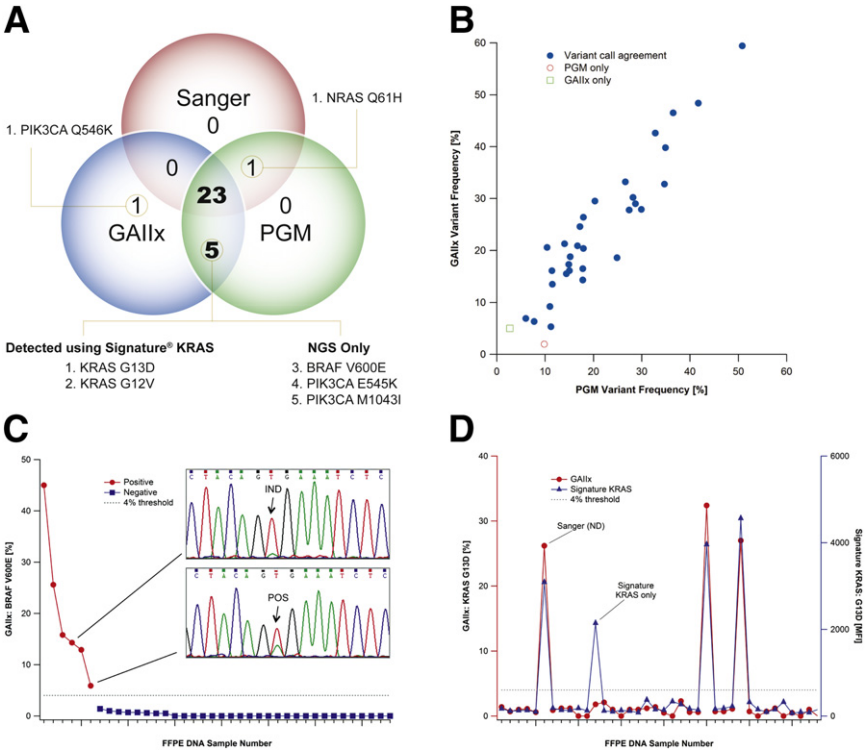


**Figure 6** Positive NGS call summary comparing results by platform and with Sanger sequencing and Signature KRAS analysis. **A**: A Venn diagram distribution of 29 positive variant calls across NGS and Sanger sequencing of KRAS, BRAF, and PIK3CA regions. Five variant calls in agreement between the GAIIx and PGM platforms were indeterminate using Sanger sequencing. One unique call of PIK3CA Q546K was detected only on the GAIIx. **B**: Variant frequency comparison of GAIIx calls (*y* axis) versus PGM calls (*x* axis) for positive calls higher than a 4% threshold. **C**: GAIIx of BRAF V600E showing percentage variant in descending order and delineation of positive and negative calls for 38 FFPE DNA samples. Example sequencing electropherograms are shown (**inset panels**) comparing a sample detected with 17.3% V600E but indeterminate (IND) by Sanger (**top inset panel**). This result was contrasted with a separate sample in which BRAF V600E was detected at 5.9% but positive (POS) by Sanger (**bottom inset panel**). **D**: KRAS G13D analysis using GAIIx and Signature KRAS showing percentage variant (left axis) compared with median fluorescence intensity (right axis) across 38 CRC FFPE samples. Labels for two samples indicate one sample detected by both Signature KRAS and NGS but indeterminate by Sanger and another sample detected using only Signature KRAS. Samples were not sorted in the same order between **C** and **D**.

for all nucleotide positions, which is consistent with at least one previous report.[35]

A better understanding of the error models for targeted high-depth NGS methods of FFPE specimens, combined with more sophisticated bioinformatic algorithms for low-level variant detection, is needed to realize the clinical value of ultradeep sequencing at the lower bound of analytical sensitivity. Our initial threshold of 4% was established from three FFPE specimens and an analytical titration of three others (Figure 5) to optimize sensitivity and positive predictive value. Also, not all FFPE specimens are equivalent for NGS assessments. In our study of 39 FFPE specimens sourced from 10- to 14-year-old blocks, one sample failed read-quality metrics and another yielded five variant calls across the 1.3 kb of enriched sequence content. Of these, three variants were associated with G>A or C>T transitions at 4% to 7% abundance. Routine clinical testing of FFPE samples should recognize the potentially variable impact of different FFPE samples on enrichment and NGS outputs and, in particular, high-sensitivity mutation detection. We expect that the thresholds for variant calling can be adjusted for some sample cohorts, consistent with their collection, processing, and storage conditions.[36] Moreover, a careful study of FFPE blocks sourced from different preparation and storage conditions is needed to refine call algorithms and thresholds and identify preanalytical criteria predictive of higher-background variation.

This said, we generally find that FNA samples were well suited for NGS analysis, particularly when using targeted, multiplexed panels with low DNA input requirements (≤10 ng) that can accommodate the poor nucleic acid yields that may be obtained from such biopsy specimens. The integration of a quality control process before NGS analysis can help identify lower quality samples before NGS analysis, and the incorporation of rigorously characterized positive controls, such as the pooled cell line control evaluated in this study, can ensure more reliable performance for each run and support proficiency testing in the clinical laboratory. Consequently, we routinely incorporate a pooled cell line control and an adequate reference cell line DNA sample, such as NA12878 from the Coriell Repository, as process controls.

**Table 3** Platform Agreement Matrix Comparing GAIIx/PGM Analysis with Sanger Sequencing and Signature KRAS for 38 FFPE DNA Samples from Colorectal Tumor Resections

| | Sanger sequencing | | Signature KRAS | |
|---|---|---|---|---|
| | Positive | Negative | Positive | Negative |
| GAIIx and (PGM) | | | | |
| Positive | 23 | 6 (5)* | 15 | 0 |
| Negative | 0 | 123 (124)* | 1† | 250 |
| Accuracy (%) | 96.1 (92.5—98.9) | | 99.6 (97.9—100) | |
| Sensitivity (%) | 100 (85.2—100) | | 93.8 (69.8—99.8) | |
| Specificity (%) | 95.3 (90.2—98.3) | | 100 (98.5—100) | |

*On the PGM, one call of PIK3CA Q546K that was detected on the GAIIx was not detected by either the PGM or Sanger sequencing.

†Sample detected as KRAS G13D using Signature KRAS, but lower than variant call thresholds on both the GAIIx and PGM.

**Table 4** NGS Platform and Sanger Sequencing Analysis of Thyroid FNA Specimens Relative to Cytological Data

| | | GAIIx | | | PGM | | |
|---|---|---|---|---|---|---|---|
| ID | FNA cytological data | Variant | Reads | Frequency (%) | Variant | Reads | Frequency (%) |
| B-054 | Malignant | BRAF V600E | 22022 | 14 | BRAF V600E | 13413 | 7 |
| B-072 | Malignant | BRAF V600E | 12529 | 35 | BRAF V600E | 10363 | 24 |
| B-075 | Malignant | BRAF V600E | 22867 | 21 | BRAF V600E | 8067 | 13 |
| B-012 | Suspicious | HRAS G13R* | 5760 | 23 | HRAS G13R | 6805 | 22 |
| B-051 | Suspicious | HRAS Q61R | 5187 | 35 | HRAS Q61R | 12649 | 36 |
| B-046 | Malignant | NRAS Q61R | 24447 | 45 | NRAS Q61R | 1261 | 43 |
| B-022 | Malignant | Neg. | | | Neg. | | |
| B-009B | Benign | Neg. | | | Neg. | | |
| B-071A | Benign | Neg. | | | Neg. | | |
| B-036A | Benign | KRAS G13D_KRAS V14I† | 7420 | 7 | Neg. | | |

* HRAS G13R (c.37 G>C) is a less common thyroid-associated variant confirmed with Sanger sequencing.

† KRAS G13D_V14I (c.38_40 GCG>ACA) is a putative rare mutation in KRAS, not confirmed by either sequencing or PGM analysis. The compound variant was detected in 7% of reads. An additional 3% of reads had only the V14I variant.

Neg., mutation negative, no variants detected within the sequenced regions.

More important, the two-step tagging PCR and NGS procedure overcomes limitations associated with Sanger sequencing or probe-based methods. Sanger sequencing has a limited analytical sensitivity of approximately 15% to 20%[37,38] and a reported 11.1% false positive and 6.1% false negative rate using automated scoring.[39] Indeed, this study confirms that some mutations that are detected by independent NGS platforms are missed by conventional sequencing but detected by a more sensitive liquid bead array method.[17] Of six indeterminate calls by Sanger sequencing, five variants were detected on both platforms, two of which overlapped with the probe designs on the liquid bead mutation detection assay and were subsequently confirmed. In one sample, a KRAS G13D variant was detected using the liquid bead array, but below the variant calling threshold of both NGS platforms (Figure 6D). This result reflected the greater sensitivity at lower input variant but nonlinear response of this probe-based assay. Even so, the value of broad sequence analysis across 1283 bp in 35 amplicons, or even 487 bp in nine amplicons, was exemplified by the detection of uncommon mutations in both FFPE (eg, KRAS A146T and NRAS Q61H) and FNA DNA (eg, HRAS G13R). Less common mutations, such as these, are either too infrequent to justify Sanger sequencing in every sample or not included in the original probe design for the bead array assay. Even in the case of improved methods based on novel PCR enrichment strategies, such as COLD-PCR,[40,41] or the use of blocking primers that preferentially amplify the mutant sequence, the throughput of these techniques is limiting and requires excessive DNA to interrogate many different targets.

Although the DNA input for the larger 35-amplicon enrichment panel would still appear modest (approximately 50 ng), even this input can be limiting for some sample sets. For example, in a recent study of >100 FFPE tumor biopsy specimens, every sample provided ample DNA for PCR using the more targeted 9-amplicon panel. Yet, 24% of these samples failed to provide sufficient DNA for quality control and enrichment, using the larger 35-amplicon panel (data not shown). Such yield constraints may be particularly acute for FFPE slides with scant tumor burden or cell equivalents and/or those for which DNA must be carefully spared for confirmation testing, assessments of other markers, or additional studies. As a result, a focused panel that is designed to confirm mutations identified from screening assays or is generated to target mutations represented in high diagnostic yield in the sample population of interest offers significant operational and performance advantages that are practically realized in our results.

The two NGS platforms described in this study provide complementary capabilities for mutation profiling and confirmatory detection suitable to the clinical laboratory environment. Quantification of cancer gene mutations was both accurate and highly correlated (Table 2) when the same PCR enrichment strategy was compared across the two NGS instruments (1% to 35% mutation incidence; 16-gene panel on the GAIIx compared with the PGM). The GAIIx yielded higher read quality and longer reads, with far greater sequencing output and sample throughput than the PGM. For example, our results indicate that a single-flow cell lane of the GAIIx can support a median read depth of at least 1000 times for up to 768 samples processed using the 16-gene PCR enrichment panel. In fact, we have processed as many as 394 samples in a single GAIIx run. However, the scale of the upfront sample preparation and longer turnaround time for this sequencing is relatively inefficient for conventional molecular diagnostics. In contrast, the PGM system offers much faster turnaround times while still supporting sample multiplexing and is suitable for focused cancer-specific enrichment panels. We successfully evaluated 20 samples per 316 chips with a five-gene panel and achieved complete analysis of the 39 FFPE and 10 FNA specimens in three chip runs performed in a single day. Hardware options for rapid sequencing are also supported by emerging systems, such as the MiSeq personal sequencer, and further improvements in the PGM system are

being rapidly realized through both upgraded reagents and software.

The NGS work flows we describe herein offer the ability to screen many cancer-relevant genes and then rapidly confirm mutations in targeted subsets of genes. This capability is particularly appealing given the distinct sequencing chemistries used by the GAIIx and PGM platforms and the high degree of qualitative and quantitative concordance with variant standards and previously genotyped residual clinical specimens. Combined with an independent method for target enrichment, this orthogonal detection can provide a solution for the conundrum of how to validate clinically actionable mutations from NGS, particularly low-abundance mutations. For example, there were five variants (Figure 6A) that were detected in separate samples on the GAIIx and PGM platforms, but were indeterminate by Sanger sequencing. High-depth sequencing on either NGS platform can detect such low-level variants. Such confirmation capabilities are expected to be even more powerful across the PGM and MiSeq given that both of these instruments are capable of rapid sequencing and can be leveraged to identify options for individualized therapy within the needed timeframe for clinical actionable intervention.

NGS technology can interrogate many features, including both clinically actionable and emerging markers, while also uniting the qualitative and quantitative needs of diagnostic testing. The results of our study demonstrate the potential for highly sensitive detection of drugable mutations in clinically relevant tumor samples and establish a precedent for comparable work flows that can address current limitations in cancer molecular diagnostics, including the confirmation of detected variants across platforms. With the inevitable development of sample prequalification and stepwise process quality control metrics, standardization of data analysis methods, and the availability of rigorously defined proficiency standards, such technologies will likely become routine for clinical sample testing in the future.

## Acknowledgments

We thank Fei Ye and Emmanuel Labourier for assessing the CRC specimens using the Signature assay, Maura Lloyd for assisting with preparation and qualification of the thyroid specimens, and Annette Schlageter for providing feedback and assisting with drafting the manuscript.

## Supplemental Data

Supplemental material for this article can be found at *http://dx.doi.org/10.1016/j.jmoldx.2012.11.006*.

## References

1. Harismendy O, Schwab RB, Bao L, Olson J, Rozenzhak S, Kotsopoulos SK, Pond S, Crain B, Chee MS, Messer K, Link DR, Frazer KA: Detection of low prevalence somatic mutations in solid tumors with ultra-deep targeted sequencing. Genome Biol 2011, 12: R124
2. Kohlmann A, Klein HU, Weissmann S, Bresolin S, Chaplin T, Cuppens H, Haschke-Becher E, Garicochea B, Grossmann V, Hanczaruk B, Hebestreit K, Gabriel C, Iacobucci I, Jansen JH, Te Kronnie G, van de Locht L, Martinelli G, McGowan K, Schweiger MR, Timmermann B, Vandenberghe P, Young BD, Dugas M, Haferlach T: The Interlaboratory RObustness of Next-generation sequencing (IRON) study: a deep sequencing investigation of TET2, CBL and KRAS mutations by an international consortium involving 10 laboratories. Leukemia 2011, 25:1840−1848
3. Thomas RK, Nickerson E, Simons JF, Janne PA, Tengs T, Yuza Y, Garraway LA, LaFramboise T, Lee JC, Shah K, O'Neill K, Sasaki H, Lindeman N, Wong KK, Borras AM, Gutmann EJ, Dragnev KH, DeBiasi R, Chen TH, Glatt KA, Greulich H, Desany B, Lubeski CK, Brockman W, Alvarez P, Hutchison SK, Leamon JH, Ronan MT, Turenchalk GS, Egholm M, Sellers WR, Rothberg JM, Meyerson M: Sensitive mutation detection in heterogeneous cancer specimens by massively parallel picoliter reactor sequencing. Nat Med 2006, 12: 852−855
4. Jones SJ, Laskin J, Li YY, Griffith OL, An J, Bilenky M, Butterfield YS, Cezard T, Chuah E, Corbett R, Fejes AP, Griffith M, Yee J, Martin M, Mayo M, Melnyk N, Morin RD, Pugh TJ, Severson T, Shah SP, Sutcliffe M, Tam A, Terry J, Thiessen N, Thomson T, Varhol R, Zeng T, Zhao Y, Moore RA, Huntsman DG, Birol I, Hirst M, Holt RA, Marra MA: Evolution of an adenocarcinoma in response to selection by targeted kinase inhibitors. Genome Biol 2010, 11:R82
5. De Roock W, Claes B, Bernasconi D, De Schutter J, Biesmans B, Fountzilas G, et al: Effects of KRAS, BRAF, NRAS, and PIK3CA mutations on the efficacy of cetuximab plus chemotherapy in chemotherapy-refractory metastatic colorectal cancer: a retrospective consortium analysis. Lancet Oncol 2010, 11:753−762
6. Nikiforova MN, Nikiforov YE: Molecular diagnostics and predictors in thyroid cancer. Thyroid 2009, 19:1351−1361
7. Huijsmans CJ, Damen J, van der Linden JC, Savelkoul PH, Hermans MH: Comparative analysis of four methods to extract DNA from paraffin-embedded tissues: effect on downstream molecular applications. BMC Res Notes 2010, 3:239
8. Gerlinger M, Rowan AJ, Horswell S, Larkin J, Endesfelder D, Gronroos E, Martinez P, Matthews N, Stewart A, Tarpey P, Varela I, Phillimore B, Begum S, McDonald NQ, Butler A, Jones D, Raine K, Latimer C, Santos CR, Nohadani M, Eklund AC, Spencer-Dene B, Clark G, Pickering L, Stamp G, Gore M, Szallasi Z, Downward J, Futreal PA, Swanton C: Intratumor heterogeneity and branched evolution revealed by multiregion sequencing. N Engl J Med 2012, 366:883−892
9. Nowell PC: Mechanisms of tumor progression. Cancer Res 1986, 46: 2203−2207
10. Szerlip NJ, Pedraza A, Chakravarty D, Azim M, McGuire J, Fang Y, Ozawa T, Holland EC, Huse JT, Jhanwar S, Leversha MA, Mikkelsen T, Brennan CW: Intratumoral heterogeneity of receptor tyrosine kinases EGFR and PDGFRA amplification in glioblastoma defines subpopulations with distinct growth factor response. Proc Natl Acad Sci U S A 2012, 109:3041−3046
11. Yancovitz M, Litterman A, Yoon J, Ng E, Shapiro RL, Berman RS, Pavlick AC, Darvishian F, Christos P, Mazumdar M, Osman I, Polsky D: Intra- and inter-tumor heterogeneity of BRAF(V600E) mutations in primary and metastatic melanoma. PLoS One 2012, 7: e29336
12. Taniguchi K, Okami J, Kodama K, Higashiyama M, Kato K: Intratumor heterogeneity of epidermal growth factor receptor mutations in lung cancer and its correlation to the response to gefitinib. Cancer Sci 2008, 99:929−935
13. Metzker ML: Sequencing technologies: the next generation. Nat Rev Genet 2010, 11:31−46

14. Rothberg JM, Hinz W, Rearick TM, Schultz J, Mileski W, Davey M, et al: An integrated semiconductor device enabling non-optical genome sequencing. Nature 2011, 475:348−352
15. MacConaill LE, Campbell CD, Kehoe SM, Bass AJ, Hatton C, Niu L, Davis M, Yao K, Hanna M, Mondal C, Luongo L, Emery CM, Baker AC, Philips J, Goff DJ, Fiorentino M, Rubin MA, Polyak K, Chan J, Wang Y, Fletcher JA, Santagata S, Corso G, Roviello F, Shivdasani R, Kieran MW, Ligon KL, Stiles CD, Hahn WC, Meyerson ML, Garraway LA: Profiling critical cancer gene mutations in clinical tumor samples. PLoS One 2009, 4:e7887
16. Forbes SA, Tang G, Bindal N, Bamford S, Dawson E, Cole C, Kok CY, Jia M, Ewing R, Menzies A, Teague JW, Stratton MR, Futreal PA: COSMIC (the Catalogue of Somatic Mutations in Cancer): a resource to investigate acquired mutations in human cancer. Nucleic Acids Res 2010, 38:D652−D657
17. Laosinchai-Wolf W, Ye F, Tran V, Yang Z, White R, Bloom K, Choppa P, Labourier E: Sensitive multiplex detection of KRAS codons 12 and 13 mutations in paraffin-embedded tissue specimens. J Clin Pathol 2011, 64:30−36
18. Frank DN: BARCRAWL and BARTAB: software tools for the design and implementation of barcoded primers for highly multiplexed DNA sequencing. BMC Bioinformatics 2009, 10:362
19. Li H, Durbin R: Fast and accurate short read alignment with Burrows-Wheeler transform. Bioinformatics 2009, 25:1754−1760
20. DePristo MA, Banks E, Poplin R, Garimella KV, Maguire JR, Hartl C, Philippakis AA, del Angel G, Rivas MA, Hanna M, McKenna A, Fennell TJ, Kernytsky AM, Sivachenko AY, Cibulskis K, Gabriel SB, Altshuler D, Daly MJ: A framework for variation discovery and genotyping using next-generation DNA sequencing data. Nat Genet 2011, 43:491−498
21. Duncavage EJ, Magrini V, Becker N, Armstrong JR, Demeter RT, Wylie T, Abel HJ, Pfeifer JD: Hybrid capture and next-generation sequencing identify viral integration sites from formalin-fixed, paraffin-embedded tissue. J Mol Diagn 2011, 13:325−333
22. Kerick M, Isau M, Timmermann B, Sültmann H, Herwig R, Krobitsch S, Schaefer G, Verdorfer I, Bartsch G, Klocker H, Lehrach H, Schweiger MR: Targeted high throughput sequencing in clinical cancer settings: formaldehyde fixed-paraffin embedded (FFPE) tumor tissues, input amount and tumor heterogeneity. BMC Med Genomics 2011, 4:68
23. Wagle N, Berger MF, Davis MJ, Blumenstiel B, DeFelice M, Pochanard P, Ducar M, Van Hummelen P, MacConaill LE, Hahn WC, Meyerson M, Gabriel SB, Garraway LA: High-throughput detection of actionable genomic alterations in clinical tumor samples by targeted, massively parallel sequencing. Cancer Disc 2012, 2:82−93
24. Mellmann A, Harmsen D, Cummings CA, Zentz EB, Leopold SR, Rico A, Prior K, Szczepanowski R, Ji Y, Zhang W, McLaughlin SF, Henkhaus JK, Leopold B, Bielaszewska M, Prager R, Brzoska PM, Moore RL, Guenther S, Rothberg JM, Karch H: Prospective genomic characterization of the German enterohemorrhagic Escherichia coli O104:H4 outbreak by rapid next generation sequencing technology. PLoS One 2011, 6:e22751
25. Howden BP, McEvoy CR, Allen DL, Chua K, Gao W, Harrison PF, Bell J, Coombs G, Bennett-Wood V, Porter JL, Robins-Browne R, Davies JK, Seemann T, Stinear TP: Evolution of multidrug resistance during Staphylococcus aureus infection involves mutation of the essential two component regulator WalKR. PLoS Pathog 2011, 7: e1002359
26. Loman NJ, Misra RV, Dallman TJ, Constantinidou C, Gharbia SE, Wain J, Pallen MJ: Performance comparison of benchtop high-throughput sequencing platforms. Nat Biotechnol 2012, 30: 434−439
27. Mamanova L, Coffey AJ, Scott CE, Kozarewa I, Turner EH, Kumar A, Howard E, Shendure J, Turner DJ: Target-enrichment strategies for next-generation sequencing. Nat Methods 2010, 7:111−118
28. Valencia CA, Rhodenizer D, Bhide S, Chin E, Littlejohn MR, Keong LM, Rutkowski A, Bonnemann C, Hegde M: Assessment of target enrichment platforms using massively parallel sequencing for the mutation detection for congenital muscular dystrophy. J Mol Diagn 2012, 14:233−246
29. van Beers EH, Joosse SA, Ligtenberg MJ, Fles R, Hogervorst FB, Verhoef S, Nederlof PM: A multiplex PCR predictor for aCGH success of FFPE samples. Br J Cancer 2006, 94:333−337
30. Stowers CC, Haselton FR, Boczko EM: An analysis of quantitative PCR reliability through replicates using the Ct method. J Biomed Sci Eng 2010, 3:459−469
31. Molinari F, Felicioni L, Buscarino M, De Dosso S, Buttitta F, Malatesta S, Movilia A, Luoni M, Boldorini R, Alabiso O, Girlando S, Soini B, Spitale A, Di Nicolantonio F, Saletti P, Crippa S, Mazzucchelli L, Marchetti A, Bardelli A, Frattini M: Increased detection sensitivity for KRAS mutations enhances the prediction of anti-EGFR monoclonal antibody resistance in metastatic colorectal cancer. Clin Cancer Res 2011, 17:4901−4914
32. Parker WT, Lawrence RM, Ho M, Irwin DL, Scott HS, Hughes TP, Branford S: Sensitive detection of BCR-ABL1 mutations in patients with chronic myeloid leukemia after imatinib resistance is predictive of outcome during subsequent therapy. J Clin Oncol 2011, 29: 4250−4259
33. Zhou Q, Zhang XC, Chen ZH, Yin XL, Yang JJ, Xu CR, Yan HH, Chen HJ, Su J, Zhong WZ, Yang XN, An SJ, Wang BC, Huang YS, Wang Z, Wu YL: Relative abundance of EGFR mutations predicts benefit from gefitinib treatment for advanced non-small-cell lung cancer. J Clin Oncol 2011, 29:3316−3321
34. Molinari F, Felicioni L, Buscarino M, De Dosso S, Buttitta F, Malatesta S, Movilia A, Luoni M, Boldorini R, Alabiso O, Girlando S, Soini B, Spitale A, Di Nicolantonio F, Saletti P, Crippa S, Mazzucchelli L, Marchetti A, Bardelli A, Frattini M: Increased detection sensitivity for KRAS mutations enhances the prediction of anti-EGFR monoclonal antibody resistance in metastatic colorectal cancer. Clin Cancer Res 2011, 17:4901−4914
35. Su KY, Chen HY, Li KC, Kuo ML, Yang JC, Chan WK, Ho BC, Chang GC, Shih JY, Yu SL, Yang PC: Pretreatment epidermal growth factor receptor (EGFR) T790M mutation predicts shorter EGFR tyrosine kinase inhibitor response duration in patients with non-small-cell lung cancer. J Clin Oncol 2012, 30:433−440
36. Forshew T, Murtaza M, Parkinson C, Gale D, Tsui DW, Kaper F, Dawson SJ, Piskorz AM, Jimenez-Linan M, Bentley D, Hadfield J, May AP, Caldas C, Brenton JD, Rosenfeld N: Noninvasive identification and monitoring of cancer mutations by targeted deep sequencing of plasma DNA. Sci Transl Med 2012, 4:136ra68
37. Bar-Eli M, Ahuja H, Gonzalez-Cadavid N, Foti A, Cline MJ: Analysis of N-RAS exon-1 mutations in myelodysplastic syndromes by polymerase chain reaction and direct sequencing. Blood 1989, 73: 281−283
38. Collins SJ, Howard M, Andrews DF, Agura E, Radich J: Rare occurrence of N-ras point mutations in Philadelphia chromosome positive chronic myeloid leukemia. Blood 1989, 73:1028−1032
39. Tsiatis AC, Norris-Kirby A, Rich RG, Hafez MJ, Gocke CD, Eshleman JR, Murphy KM: Comparison of Sanger sequencing, pyrosequencing, and melting curve analysis for the detection of KRAS mutations: diagnostic and clinical implications. J Mol Diagn 2010, 12: 425−432
40. Mancini I, Santucci C, Sestini R, Simi L, Pratesi N, Cianchi F, Valanzano R, Pinzani P, Orlando C: The use of COLD-PCR and high-resolution melting analysis improves the limit of detection of KRAS and BRAF mutations in colorectal cancer. J Mol Diagn 2011, 12: 705−711
41. Milbury CA, Li J, Makrigiorgos GM: Ice-COLD-PCR enables rapid amplification and robust enrichment for low-abundance unknown DNA mutations. Nucleic Acids Res 2011, 39:e2